

PRIMARY STUDY OF PLASTIC MICRO FIBRE WASTE FOR SOUND ABSORPTION APPLICATIONS

Tomas ASTRAUSKAS^{id*}, Mantas PRANSKEVIČIUS^{id}, Tomas JANUŠEVIČIUS^{id}

*Research Institute of Environmental Protection,
Vilnius Gediminas Technical University, Saulėtekio al. 11, Vilnius, Lithuania*

Received 16 January 2023; accepted 20 February 2023

Abstract. Plastic and waste production has increased significantly in recent years. According to the various predictions the plastic production is not slowing down in the near future. Since 1960, plastic production has risen to 322 million tonnes in 2015 and expected to double in the next 20 years (Lusher et al., 2017). According to the 2020 statistical data, the leading sectors in plastic demand are packaging, building and construction, with 40.5% and 20.4% respectively. In 2019, an estimated 41% of plastic packaging waste was recycled in the EU. Despite the advantages of plastic recycling technologies, there are also a number of problems. Mechanical recycling refers to the processing of plastics waste into secondary raw material or products without significantly changing the material's chemical structure. In this paper, we focused at the problem of plastic micro fibre (PMF) waste, which generated during mechanical recycling. The possibilities of using PMF for sound absorption applications are tested. For primary acoustic characterisation PMF was not treated thermally or bound using other materials. The controlled parameter of the material is density. The density of material changed from 100 to 300 kg/m³. The PMF sound absorption characterisation was performed using standard transfer function method (ISO 10534-2). The acoustic performance of materials predicted with acoustic porous materials Delany-Bazley-Miki model. The aim of this paper is to gain the essential knowledge about the plastic micro fibre sound absorption performance to find the possible recycling application for sound absorption.

Keywords: sound absorption, waste, plastic micro fibres, density, air flow resistivity.

Introduction

Plastic production has increased significantly over the last decades and unfortunately this trend is not slowing down. Since 1960, plastic production has risen to 322 million tonnes in 2015 and is expected to double in the next 20 years (Lusher et al., 2017). Around 25.8 million tonnes of plastic waste are generated in Europe every year (EUROPARC Federation, 2018). Less than 30% of this waste is collected for recycling. A large part of this volume is shipped out of the EU for treatment in third countries where different environmental standards may apply (European Commission, 2018).

Almost 90% of plastics production uses primary fossil fuels. This accounts for up to 6% of the world's oil consumption. With the growing demand for plastics, this demand is expected to rise to 20% by 2050 (European Parliament, 2017). Here again, recycling of plastics becomes very important, not only because of the need for virgin material, but also because of environmental pollution such as incineration.

It is estimated that the production of plastics and the incineration of plastic waste emit around 400 million tonnes of CO₂ annually worldwide (European Commission, 2018). Using more recycled plastics can reduce dependence on fossil fuel extraction for plastics production and reduce CO₂ emissions (FEDEREC, 2017).

According to 2019 data, up to 34.4 kg of packaging plastic waste is generated per European and only about 14.1 kg of this amount is recycled (Eurostat, 2021). However, it should not be forgotten that in Europe the vast majority of plastic waste is still landfilled or incinerated (31% and 39% respectively); in the last decade, there has been a decrease in the amount of plastic landfilled and an increase in the amount incinerated (EUROPARC Federation, 2018).

According to the 2020 statistics, the leading sectors in terms of plastic demand by sector are packaging and building and construction, with 40.5% and 20.4% respectively. Automation accounts for 8.8%, while electronics and electrical installation accounts for 6.2%. Household, leisure and sports account for – 4.3%. Agriculture

* Corresponding author. E-mail: tomas.astrauskas@vilniustech.lt

accounts for up to 3.2% of plastic demand. Other sectors also account for a significant share of plastic demand, totalling up to 16.6%.

Despite the advantages of plastic recycling technologies, there are also a number of problems. The mechanical recycling process starts with the shredding of the plastic. The shredded particles travel up to the first washing stage via a conveyor. In this stage, heavy impurities such as glass, soil, metals, etc. are removed from the flow by gravity (Soto et al., 2020). After the primary cleaning, a secondary cleaning follows, focusing on the cleaning of the plastic surface. In this stage, a friction washer is used to remove organic residues, adhesives and label residues from the plastic surface. This stage generates large quantities of industrial waste water, which is contaminated with micro plastic particles and creates toxicological risks for aquatic ecosystems. Other problems are also encountered at this stage. One of them is the formation of plastic-contaminated microfiber pulp. The recovery of this plastic waste is becoming an unsolvable issue. The most common fate of this material is landfilling. In literature, there are very few studies that have analysed in depth the washing process of post-consumer plastic film waste as an essential step in its mechanical recycling (Perrone, 1988; Soto et al., 2020).

Number of studies work on recycled plastics for sound absorption application. The plastic waste often incorporated in different composite materials. In most of the studies various plastic waste is incorporated in composite materials as the supplementary material, for example in concrete (Boucedra et al., 2020), hemp (Wang et al., 2022a, 2022b) or other. The alternative option to use recycled plastics for production of the acoustic metamaterials. These materials rely on plastics as a material which is easy to manipulate, especially using 3D printing technologies (Naimušin & Januševičius, 2023). In most cases various resonators or other symmetrical pore structure materials are being printed and tested for sound absorption applications (Li et al., 2023; Z. Wang et al., 2023).

As mentioned before plastic micro fibres was not researched as the main material for application purposes. In this paper the PMF is researched for sound absorption applications. The aim of this paper is to get knowledge about PMF sound absorption as well as test known acoustic models for PMF sound absorption prediction. The article is organised as follows: in Section 2 the methods and materials used in the study are presented, Section 3 presents the main results and discussion, and in Section 4 the conclusions and future prospects are presented.

Materials and methods

In this section the methods of this study presented. In this study the experimental and theoretical techniques were used to characterize the acoustic and non-acoustic properties of PMF. Experimental techniques include transfer function method for sound absorption determination according ISO 10534-2 and air flow resistivity determination according ISO 9053-1. The theoretical study was performed using two acoustic Horoshenkov – Swift and Delany – Bazley – Miki models which are used for porous materials sound absorption prediction.

Sample preparation method

In this section the sample preparation method is presented. As the raw material PMF was used. The PMF was obtained from plastic recycling company. The PMF was dried for 24 hours in 80 ± 3 °C without mixing. After drying in was noticed that PMF was stuck together which would affect the sound absorption properties. To separate the PMF the blender was used. The bulk density of dried PMF was 82.0 ± 3.5 kg/m³, and after blending 39.6 ± 2.3 kg/m³.

Even in Figure 1 can be seen with naked eye that blended PMF (Figure 1b) is less dense compared with not blended PMF (Figure 1a). Such sample preparation

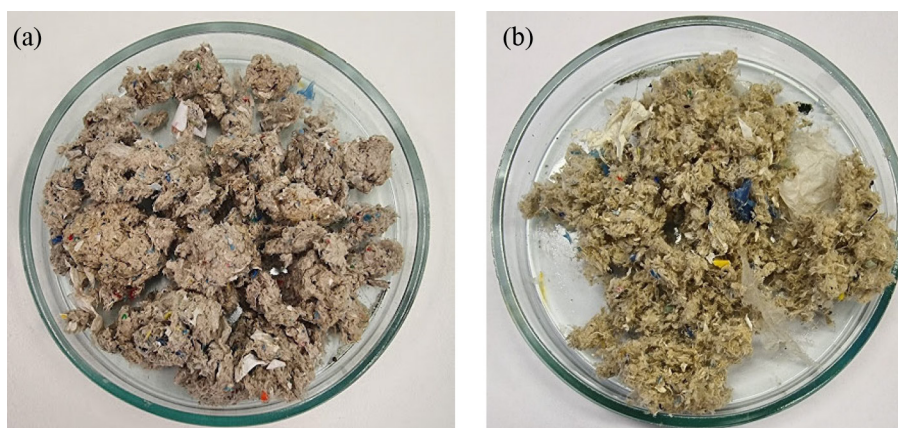


Figure 1. Raw PMF used in the study: (a) Dried PMF without blending; (b) blended PMF

production according to porous material acoustic models, should lead to higher porosity values, thus higher sound absorption capability.

The blended PMF was used further in this study. The grain size analysis was performed.

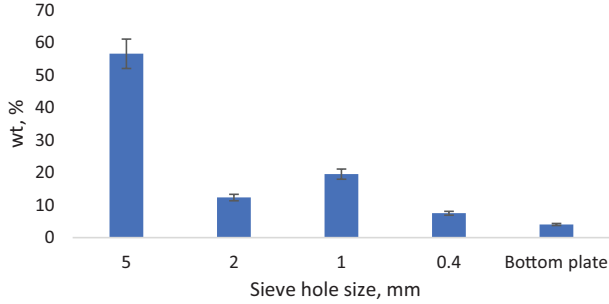


Figure 2. Granulometric composition of PMF

In the Figure 2 the granulometric composition of PMF presented. The results show that most of the particles in blended PMF hold in sieve with 5 mm grains (56.6 wt,%) and 1 mm (19.3 wt,%). The other particle sizes showed less than percentage 2 mm (56.6 wt,%), 0.4 mm (7.5 wt,%) in the bottom plate was found least PMF (4.0 wt,%).

Transfer function method

To obtain the sound absorption coefficient (SAC) of the PMF, the ISO 10534-2 standard method was used (International Organization for Standardization [ISO], 2001). Such method was chosen due to the requirements for sample size compared with methods which can be performed in reverberant rooms. Three microphone impedance tube measurement system was used for this study. The cross section of the tube was circular with a diameter of 30 mm. The samples were rigidly backed. The experimental setup is shown in Figure 3. The distance between mic no. 1 and no. 2 $X_{12} = 120$ mm; between mic no. 2 and no. 3 $X_{23} = 20$ mm and the distance from the nearest mic to the sample $X_{3s} = 60$ mm. The diameter of the tube is 30 mm. The measured frequency range is from 250 to 4000 Hz. The results are presented using 1/3 octave band filtering. Three microphone impedance tube system work according to the same algorithm as

two microphone system but allows to do measurements quicker. Since PMF used in the study is loose, the material was put into a 3D printed sample holder. The diameter of the sample holder was 29.9 mm that inserted into the impedance tube would have no space between the holder and the tube body, while the height of the holder was 60 mm.

The transfer function method was used with three microphone technique.

The transfer function H_{12} Eq. (1) between microphone positions is calculated as the pressure ratio between pressures measured by both microphones. The transfer function for incident wave alone H_I and transfer function for reflected wave alone H_R calculated according to Eqs (2) and (3) (ISO, 2001):

$$H_{12} = \frac{P_3}{P_1}; \quad H_{23} = \frac{P_3}{P_2}; \quad (1)$$

$$H_{I(250-1000\text{ Hz})} = \frac{P_{3I}}{P_{1I}} = e^{-jk_0(x_{12}+x_{23})}, \quad (2)$$

$$H_{I(1-5\text{ kHz})} = \frac{P_{3I}}{P_{2I}} = e^{-jk_0(x_{23})};$$

$$H_{R(250-1000\text{ Hz})} = \frac{P_{3R}}{P_{1R}} = e^{jk_0(x_{12}+x_{23})}, \quad (3)$$

$$H_{R(1-5\text{ kHz})} = \frac{P_{3R}}{P_{2R}} = e^{jk_0(x_{23})}.$$

From Eq. (1), (2), and (3) the reflection coefficient of the sample can be calculated as:

$$R_{(1-5\text{ kHz})} = \frac{H_{23} - H_{I(1-5\text{ kHz})}}{H_{R(1-5\text{ kHz})} - H_{I3}} e^{2jk_0(X_{23}+X_{3s})}, \quad (4)$$

where: R is the reflection coefficient of the sample, k_0 is the wavenumber in air.

Finally, the sound absorption coefficient is calculated using the following expression:

$$\alpha = 1 - |R|^2. \quad (5)$$

In this paper, the results are presented in narrow octave band, each frequency has sound absorption value.

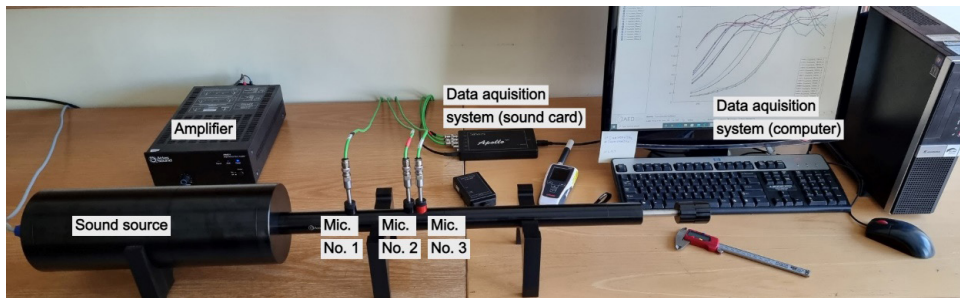


Figure 3. The impedance tube configuration for sound absorption measurements

Theoretical sound absorption prediction methods

The direct air flow method was used to determine the airflow resistivity of the materials. This method is based on the difference in air pressure between two open surfaces of material created by directional air movement. The length of the pipe must be long enough to allow close to laminar directional air flow. The sample holder consists of 50% of the cross-sectional area of evenly spaced holes. An air compressor is used to generate air pressure, and a differential manometer is used to measure the pressure difference. The air flow speed was measured with an air flow meter. The air flow speed in the device is 0.01 m/s in order to ensure that the air flow speed does not affect the difference. The method is based on the ISO 9053 standard.

To determine the air flow resistivity first the air pressure difference ΔP is measured:

$$\Delta P = P_1 - P_2, \quad (6)$$

here: ΔP air pressure difference, Pa; P_1 – air pressure in front of sample, Pa; P_2 – air pressure behind sample, Pa.

Then air flow resistance R is calculated (ISO, 1991):

$$R = \frac{\Delta P}{q_v}, \quad (7)$$

here q_v air flow rate, m^3/s .

Specific air flow resistance is calculated as multiplication between air flow resistance and cross sectional area of the sample:

$$R_s = RA, \quad (8)$$

here A – cross sectional area of the sample.

Finally, air flow resistivity is gained by dividing the specific air flow resistance by thickness of the sample:

$$\sigma = \frac{R_s}{d}, \quad (9)$$

here d – thickness of the sample, m.

The airflow resistivity is one of the main parameters non acoustic parameter for sound absorption prediction. The airflow resistivity data is used in the sound absorption prediction models.

Horoshenkov and Swift model

According to Horoshenkov and Swift of porous material model the main material parameters that determine the ability of granular material to absorb sound are airflow resistivity, grain size and porosity (Horoshenkov & Swift, 2001a, 2001b). The airflow resistivity parameter was determined experimentally. The porosity value was obtained using curve fitting method since other parameters that feed the model are known.

First the complex wave number is calculated:

$$k = \omega \sqrt{\alpha_\infty \rho_0 / \gamma P_0}, \quad (10)$$

here: k – complex wave number, ω – angular frequency rad/s,

α_∞ tortuosity, ρ_0 air density kg/m^3 $\rho_0 = 1.213 kg/m^3$ P_0 atmospheric pressure Pa $P_0 = 1.213 \times 10^5 Pa$, ratio of specific heat constants under normal conditions $\gamma = 1.4$.

The porosity values as mentioned before was obtained using curve fitting method. The porosities used in the study presented in Table 1.

The tortuosity value of the samples is calculated using formula proposed by (Umnova et al., 2005).

$$\alpha_\infty = 1 + \frac{1 - \phi}{2\phi}, \quad (11)$$

here: α_∞ tortuosity, ϕ porosity of the sample, %.

Effective density calculated according formula (Allard et al., 1989; Panneton & Olny, 2006):

$$\rho_e = k_s \rho_0 \left[1 + \frac{\sigma \varepsilon}{j \omega k_s \rho_0} \sqrt{1 + \frac{4k \alpha_\infty^2 \eta \rho_0 \omega}{\sigma^2 \Lambda^2 \varepsilon^2}} \right], \quad (12)$$

here: ρ_e effective density, α_∞ tortuosity, η dynamic viscosity of air, $\eta = 1.825 \times 10^{-5} Pa \cdot s$ Λ characteristic thermal length, m.

Then the elastic dynamic modulus of air (Sánchez-Ortiz et al., 2019):

$$K_e = \frac{\gamma P_0}{\gamma - (\gamma - 1) / \left(1 + \frac{8\eta}{j \Lambda^2 N_p \omega \rho} \sqrt{1 + \frac{j \rho \omega N_p \Lambda^2}{16\eta}} \right)}, \quad (13)$$

here: P_0 atmospheric pressure, Pa, N_p correction coefficient (0.77).

From previously calculated parameters the characteristic and specific acoustic impedances is obtained:

$$Z_c = \sqrt{K_e \rho_e}; \quad (14)$$

$$Z_s = -j \frac{Z_c}{\phi} \cot(kd), \quad (15)$$

here: Z_s specific acoustic impedance Pas/m^3 , k – complex wave number in the material, d – thickness of the sample, m.

Finally the sound reflection and absorption coefficients are obtained (Doutres et al. 2010):

$$R = \frac{\frac{z_s}{\rho_0 c_0} \cos(f) - 1}{\frac{z_s}{\rho_0 c_0} \cos(f) + 1}; \quad (16)$$

$$\alpha = 1 - |R|^2, \quad (17)$$

here: α – sound absorption coefficient, R – sound reflection coefficient.

Delany-Bazley-Miki model

This model differs from previously presented model by the fact that it uses less input parameters. The only parameter needed for the model is airflow resistivity. The model corrections proposed by (Miki, 1990) is still widely used in scientific community.

The characteristic acoustic impedance calculated according to formula:

$$Z_c = c_0 \rho_0 \left[1 + 5.5 \left(10^3 \frac{f}{\sigma} \right)^{-0.632} - j 8.43 \left(10^3 \frac{f}{\sigma} \right)^{-0.632} \right]; \quad (18)$$

$$k = \frac{\omega}{c_0} \left[1 + 7.81 \left(10^3 \frac{f}{\sigma} \right)^{-0.618} - j 11.41 \left(10^3 \frac{f}{\sigma} \right)^{-0.618} \right]; \quad (19)$$

$$Z_s = -j \frac{Z_c}{\tan(kd)}, \quad (20)$$

here: f – frequency, Hz; σ – airflow resistivity Pa·s/m².

The sound reflection and absorption is estimated using same formulas as in Horoshenkov and Swift model. The sound reflection and absorption in this model estimated using formulas no. 11 and 12.

The accuracy of both sound absorption prediction models compared with experimental data was estimated according to formula no. 15.

$$Accuracy = \sum_{n=1}^n \left[\frac{|Exp_f - Pred_f|}{Exp_f} \times 100 \right] \div n, \quad (21)$$

here: n – number of sound absorption samples within frequency domain; Exp_f – experimental sound absorption result in frequency f ; $Pred_f$ – predicted sound absorption result in frequency f .

The formula no. 15 let analyse the acoustic model accuracy, therefore allows to choose model which is more suitable for PMF sound absorption prediction.

Results and discussion

In this section the main results of the study presented. This section consists of experimental and theoretical study results and its analysis. Finally the results are discussed and compared with results gained in other studies with different materials respectively.

The samples was prepared and tested according to the methods presented in the second section. 4 different density samples was prepared and tested in this study.

In the Table 1 the main non-acoustic parameters are presented. The bulk density and airflow resistivity results was gained experimentally, but porosity results was gained using curve fitting method, by using the Horoshenkov and Swift sound absorption model.

The results in the Table 1 show that density, airflow resistivity and porosity are dependable parameters of the material. Bulk density of the samples was the controlled parameter. Lower density values results in lower airflow resistivity values while porosity is highest. Such results indicates that lower density samples have bigger air gaps between fibres, and in higher density samples it is the opposite. The values of airflow resistivity varied between 9.57 (100 kg/m³) to 227.7 (300 kg/m³) while the porosity values range from 0.75 (300 kg/m³) to 0.95 (100 kg/m³).

Table 1. The main non-acoustic parameters of the PMF samples

Sample No. 1	Bulk density*, ρ , kg/m ³		Air flow resistivity*, σ , kPa·s/m ²
1	150±1.2	0.9±0.03	44.5±2.1
2	200±1.8	0.85±0.05	63.8±3.1
3	250±2.1	0.8±0.04	143.0±7.1
4	300±2.5	0.75±0.06	227.7±11.4

Note: *Values gained experimentally. **Values gained using curve fitting method comparing with experimental results.

In the Figure 4 the sound absorption results are presented. The graphs show the predicted and experimental results of PMF of different density.

In the Figure 4 the sound absorption results are presented. The graphs show the predicted and experimental results of PMF of different density. Firstly, the results indicate that with density decrease the values of sound absorption increases, especially in higher frequency range (500 Hz and above). Such phenomenon can be justified by Airflow resistivity value decrease with density and ultimately porosity values increase. The sound absorption values of PMF in higher frequency range varied from 0.3 to 0.8, and in lower frequency range – from 0.15 to 0.5.

It is also seen that model accuracy decrease with airflow resistivity increase. The both models used in this study shows the general trend of sound absorption quite well. The Horoshenkov and Swift model showed better accuracy of 2.1 to 5.7% especially with samples with higher airflow resistivity values. The accuracy of the Delany-Bazley-Miki model varied from 5.3 to 23.5%. The prediction accuracy of both models decreases when airflow resistivity decrease. Since it is preliminary study the PMF into sample holder was put by hand which could result some minor air gaps in the material thus slightly alter the experimental results. The similar accuracy of the different models was found in (Hurrell et al., 2018).

Plastic and micro plastic waste are being studied extensively by other authors. The amount of different

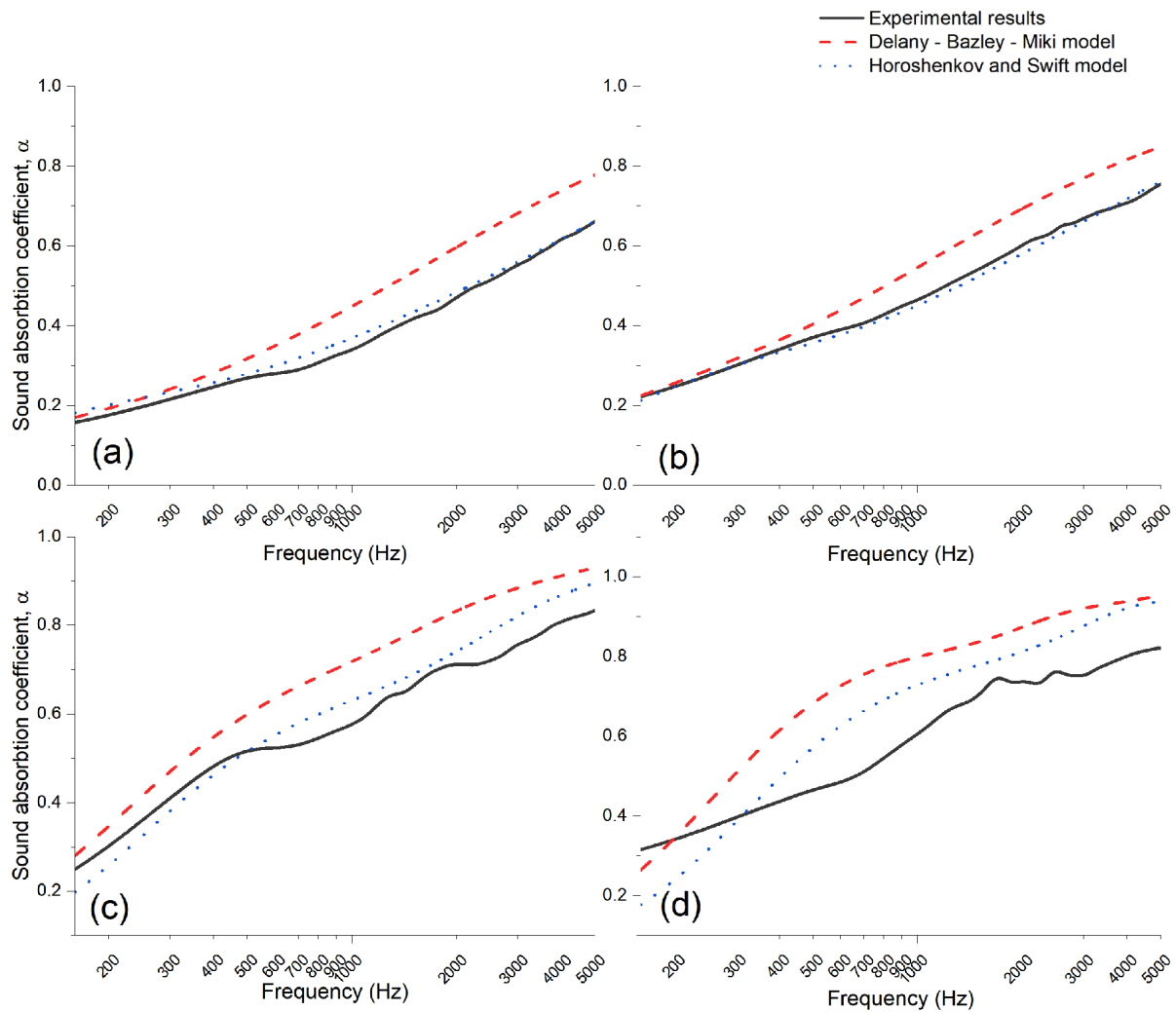


Figure 4. Experimental and predicted sound absorption results of PMF: (a) – bulk density 300 kg/m^3 ; (b) – bulk density 250 kg/m^3 ; (c) – bulk density 200 kg/m^3 ; (d) – bulk density 150 kg/m^3

studies regarding this topic shows the importance of this topic. Plastic and micro plastic studies for sound absorption applications is no exception. One of the main options of using micro plastics in the materials for sound absorption is incorporation in the composites. Authors incorporated micro plastic waste into an acoustic foam gained sound absorption coefficient up 0.99 (2100 Hz, thickness 15,9 mm) (Caniato et al., 2021). The PMF raw material at thickness of 59 mm peak sound absorption was not found due to relatively large thickness.

Conclusions

In this paper preliminary study for possible PMF applications for sound absorption was made. The results of sound absorption coefficient shows that such waste could be used as the main material in the composite for acoustic sound absorbing panel production. The sound absorption values of PMF in higher frequency (above 500 Hz) range varied from 0.3 to 0.8, and in lower frequency range – from 0.15 to 0.5.

In this study two acoustic models for prediction of sound absorption were tested to check the accuracy of the prediction when considering PMF material. The acoustic prediction model proposed by Horoshenkov and Swift was considerably more accurate compared with Delany-Bazley-Miki for PMF. The Horoshenkov-Swift model showed accuracy of 4.1%, while Delany-Bazley-Miki showed accuracy of 14.6%. In conclusion of previous statement, the prediction of PMF sound absorption results could be made more accurately using formulations proposed by Horoshenkov and Swift.

The results obtained in this study is only preliminary. Only parameters gained experimentally about the PMF was an airflow resistivity and sound absorption coefficient. In continuation of this study, micro parameters (which do influence macro parameters) need (pore size, tortuosity, porosity) to be determined. The main limitation in sound absorption prediction was that the porosity values was determined using the curve fitting method which could be not very reliable and include considerable errors.

Despite the limitations mentioned, the possible applications for sound absorption applications of PMF can be seen in the future. Future work in this study will focus on how to make the homogenous solid material. One of the main ideas to make it, is to use different binding materials, and test the sound absorption performance when considering binding material itself, binder quantity. The future composite material should be tested not only acoustically but its mechanical properties will be tested as well.

Funding

This research received no external funding.

Disclosure statement

Authors state that they do not have competing financial, professional, or personal interests from other parties.

References

- Allard, J. F., Depollier, C., & Guignouard, P. (1989). Free field surface impedance measurements of sound-absorbing materials with surface coatings. *Applied Acoustics*, 26(3), 199–207. [https://doi.org/10.1016/0003-682X\(89\)90053-4](https://doi.org/10.1016/0003-682X(89)90053-4)
- Boucedra, A., Bederina, M., & Ghernouti, Y. (2020). Study of the acoustical and thermo-mechanical properties of dune and river sand concretes containing recycled plastic aggregates. *Construction and Building Materials*, 256, 119447. <https://doi.org/10.1016/j.conbuildmat.2020.119447>
- Caniato, M., Cozzarini, L., Schmid, C., & Gasparella, A. (2021). Acoustic and thermal characterization of a novel sustainable material incorporating recycled microplastic waste. *Sustainable Materials and Technologies*, 28, e00274. <https://doi.org/10.1016/j.susmat.2021.e00274>
- Doutres, O., Salissou, Y., Atalla, N., & Panneton, R. (2010). Evaluation of the acoustic and non-acoustic properties of sound absorbing materials using a three-microphone impedance tube. *Applied Acoustics*, 71(6), 506–509. <https://doi.org/10.1016/j.apacoust.2010.01.007>
- EUROPARC Federation. (2018). *EU strategy on plastic waste – paving the way towards a circular economy*.
- European Parliament. (2017). *Strategy on plastics in the circular economy 2017. Action plan for the circular economy sub-package*. <https://www.europarl.europa.eu/legislative-train/carriage/strategy-on-plastics-in-the-circular-economy/report?sid=6601>
- European Commission. (2018). *Komisijos komunikatas Europos Parlamentui, tarybai, Europos ekonomikos ir socialinių reikalų komitetui ir regionų komitetui*. <https://eur-lex.europa.eu/legal-content/LT/TXT/HTML/?uri=CELEX:52018DC0028&from=et>
- Eurostat. (2021). *EU recycled 41% of plastic packaging waste in 2019*. <https://ec.europa.eu/eurostat/web/products-eurostat-news/-/ddn-20211027-2>
- FEDEREC. (2017). *Évaluation environnementale du recyclage en France selon la méthodologie de l'analyse de cycle de vie*. https://presse.ademe.fr/wp-content/uploads/2017/05/FEDEREC_ACV-du-Recyclage-en-France-VF.pdf
- Horoshenkov, K. V., & Swift, M. J. (2001a). The effect of consolidation on the acoustic properties of loose rubber granulates. *Applied Acoustics*, 62(6), 665–690. [https://doi.org/10.1016/S0003-682X\(00\)00069-4](https://doi.org/10.1016/S0003-682X(00)00069-4)
- Horoshenkov, K. V., & Swift, M. J. (2001b). The acoustic properties of granular materials with pore size distribution close to log-normal. *The Journal of the Acoustical Society of America*, 110(5), 2371–2378. <https://doi.org/10.1121/1.1408312>
- Hurrell, A. I., Horoshenkov, K. V., & Pelegrinis, M. T. (2018). The accuracy of some models for the airflow resistivity of nonwoven materials. *Applied Acoustics*, 130, 230–237. <https://doi.org/10.1016/j.apacoust.2017.09.024>
- International Organization for Standardization. (1991). *Acoustics – Materials for acoustical applications – Determination of airflow resistance (ISO 9053:1991)*.
- International Organization for Standardization. (2001). *Acoustics – Determination of sound absorption coefficient and impedance in impedance tubes (ISO 10534-2:2001)*.
- Li, Z., Li, X., Chua, J. W., Lim, C. H., Yu, X., Wang, Z., & Zhai, W. (2023). Architected lightweight, sound-absorbing, and mechanically efficient microlattice metamaterials by digital light processing 3D printing. *Virtual and Physical Prototyping*, 18(1), e2166851. <https://doi.org/10.1080/17452759.2023.2166851>
- Lusher, A., Hollman, P., & Mendoza-Hill, J. (2017). *Microplastics in fisheries and aquaculture: Status of knowledge on their occurrence and implications for aquatic organisms and food safety*.
- Miki, Y. (1990). Acoustical properties of porous materials. Modifications of Delany-Bazley models. *Journal of the Acoustical Society of Japan (E)*, 11(1), 19–24. <https://doi.org/10.1250/ast.11.19>
- Naimušin, A., & Januševičius, T. (2023). Development and research of recyclable composite metamaterial structures made of plastic and rubber waste to reduce indoor noise and reverberation. *Sustainability*, 15(2), 1731. <https://doi.org/10.3390/su15021731>
- Panneton, R., & Olny, X. (2006). Acoustical determination of the parameters governing viscous dissipation in porous media. *The Journal of the Acoustical Society of America*, 119(4), 2027–2040. <https://doi.org/10.1121/1.2169923>
- Perrone, C. (1988). Operating experience in a washing plant for recycled LDPE film production. *Resources, Conservation and Recycling*, 2(1), 27–36. [https://doi.org/10.1016/0921-3449\(88\)90034-1](https://doi.org/10.1016/0921-3449(88)90034-1)
- Sánchez-Orgaz, E. M., Denia, F. D., Baeza, L., & Kirby, R. (2019). Numerical mode matching for sound propagation in silencers with granular material. *Journal of Computational and Applied Mathematics*, 350, 233–246. <https://doi.org/10.1016/j.cam.2018.10.030>
- Soto, J. M., Martín-Lara, M. A., Blázquez, G., Godoy, V., Quesada, L., & Calero, M. (2020). Novel pre-treatment of dirty post-consumer polyethylene film for its mechanical recycling. *Process Safety and Environmental Protection*, 139, 315–324. <https://doi.org/10.1016/j.psep.2020.04.044>
- Umnova, O., Attenborough, K., Shin, H. C., & Cummings, A. (2005). Deduction of tortuosity and porosity from acoustic reflection and transmission measurements on thick samples of rigid-porous materials. *Applied Acoustics*, 66(6), 607–624. <https://doi.org/10.1016/j.apacoust.2004.02.005>

- Wang, H., Zhao, H., Lian, Z., Tan, B., Zheng, Y., & Erdun, E. (2022a). An optimized neural network acoustic model for porous hemp plastic composite sound-absorbing board. *Symmetry*, *14*(5), 863. <https://doi.org/10.3390/sym14050863>
- Wang, H., Zhao, H., Lian, Z., Tan, B., Zheng, Y., & Erdun, E. (2022b). Numerical simulation for porous hemp plastic composites sound absorption properties. *Journal of Materials Research and Technology*, *19*, 2458–2469. <https://doi.org/10.1016/j.jmrt.2022.05.172>
- Wang, Z., Guo, Z., Li, Z., & Zeng, K. (2023). Design, manufacture, and characterisation of hierarchical metamaterials for simultaneous ultra-broadband sound-absorbing and superior mechanical performance. *Virtual and Physical Prototyping*, *18*(1), e2111585. <https://doi.org/10.1080/17452759.2022.2111585>